A heterogeneously integrated lithium niobate-on-silicon nitride photonic platform

Mikhail Churaev(1), Rui Ning Wang(1), Annina Riedhauser(2), Viacheslav Snigirev(1), Terence Blésin(1) Charles Möhl(2), Johann Riemensberger(1), Paul Seidler(2), Tobias J. Kippenberg(1)

(1) Swiss Federal Institute of Technology Lausanne (EPFL), CH-1015 Lausanne, Switzerland, tobias.kippenberg@epfl.ch

(2) IBM Research - Europe, Säumerstrasse 4, CH-8803 Rüschlikon, Switzerland, pfs@zurich.ibm.com

Abstract *We present a $LiNbO_3$ photonic platform that heterogeneously integrates thin-film $LiNbO_3$ with Si_3N_4 photonic circuits via wafer-scale bonding. The platform achieves low propagation loss (<0.1 dB/cm) and efficient fiber-to-chip coupling (<2.5 dB per facet), enabling complex integrated photonic components with precise lithographic control.*

Introduction

Despite the recent advances in lithium niobate on insulator (LNOI) integration[1]–[4], $LiNbO_3$ photonics faces challenges that prevent its widespread adoption. First, the current fabrication of LNOI-based devices requires specific ion-beam etching that complicates the establishment of a reliable process design kit. Second, edge coupling between fibers and chips is challenging due to significant coupling loss unless more complicated double-etching techniques are used[5],[6]. Third, while record resonance quality factors have been reported in LNOI microresonators[2], losses are typically one order of magnitude higher in other reported works that provide statistical analysis. Hybrid platforms combining thin-film $LiNbO_3$ with waveguides made of Si, Si_3N_4, or Ta_2O_5 have been developed as an alternative[7]–[9], achieving electro-optic performance comparable to that of all-LNOI platforms. However, wafer-level bonding has not been demonstrated, and previous approaches aimed at specific device applications could not reveal the numerous benefits of heterogeneous integration. In this work, we demonstrate a high-yield, low-loss, integrated $LiNbO_3$-Si_3N_4 photonic platform that solves multiple issues of LNOI integrated photonics, achieved by wafer-scale heterogeneous integration of an LNOI wafer onto a patterned and planarized ultra-low-loss Si_3N_4 substrate.

Wafer-level integration approach

The process starts with the fabrication of Si3N4 waveguide structures using the photonic Damascene process[10]. The Si_3N_4 photonic Damascene process is free of crack formation in the highly tensile LPCVD Si_3N_4 film and provides high fabrication yield and ultra-low propagation loss. Direct wafer bonding is performed to the Si_3N_4 photonic integrated circuit using an additional SiO_2 interlayer deposited on the surface. The critical constraints for achieving high bonding yield, the surface roughness, and topography are measured before bonding. Both donor and acceptor wafers are coated by atomic layer deposition with a few nanometers of alumina (Al_2O_3). After optimization of the CMP treatment, the wafers are bonded and annealed at 250°C to enhance bonding strength. This way, the hybrid platform has high lithographic precision and yield, making the processing efficient for the future large-scale LNOI integration with higher throughput compared to the state-of-the-art heterogeneous die-level lithium niobate bonding approaches.

Efficient input coupling from optical fibers to photonic chips is crucial for various applications. Some recent research demonstrated the use of embedded silicon edge-couplers to overcome this issue, but in this case, the geometrical mode profile mismatch would still lead to significant coupling loss if the $LiNbO_3$ layer remained on top of underlying Si_3N_4 inverse tapers. To solve this issue, the we remove the $LiNbO_3$ slab from the coupling regions and use standard Damascene Si_3N_4 inverse tapers for efficient input coupling. However, there remains a challenge of transitioning between the regions with and without $LiNbO_3$ which is solved by implementing adiabatic tapers in the $LiNbO_3$ layer using argon ion-beam etching with a photoresist etch mask, which only affected the mode transition regions and did not impact the functional photonic components. By keeping the $LiNbO_3$ layer unprocessed for all the photonic components, we are able to achieve low optical losses through both roughness and precise align-

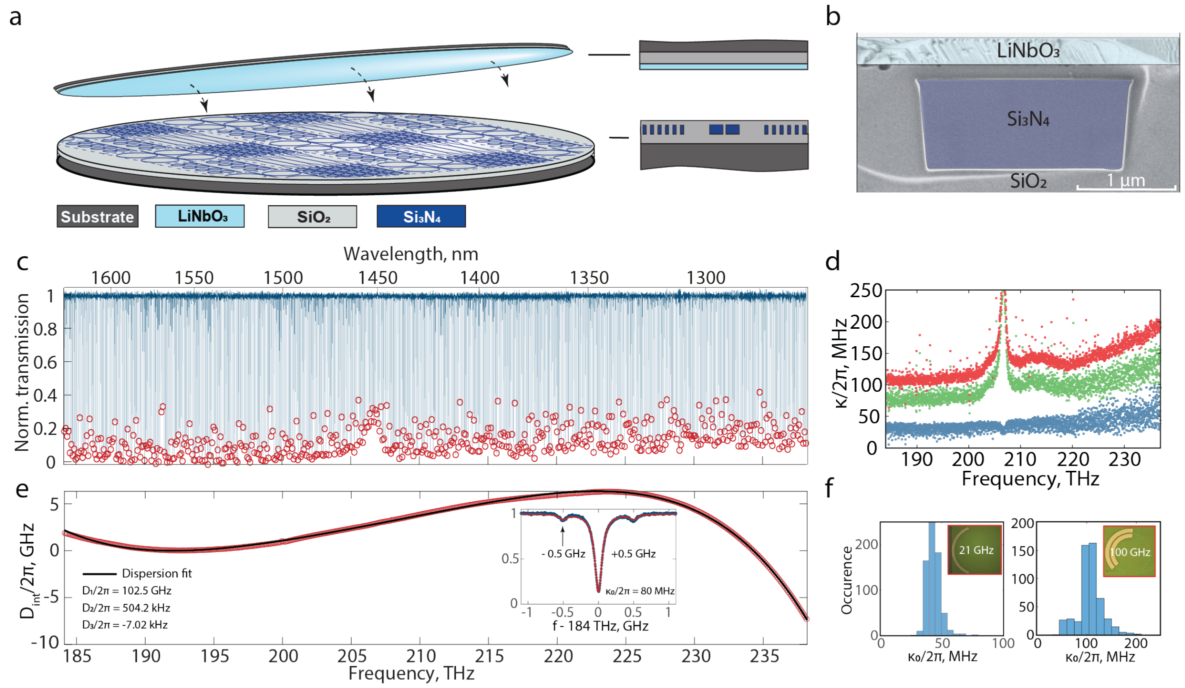

Fig. 1: (a) The hybrid approach presented in this work, involving wafer-level heterogeneous integration of thin-film $LiNbO_3$ onto Si_3N_4 integrated photonic circuits. (b) False-colored scanning electron micrograph of a cross-section of the hybrid structure. (c) Broadband spectroscopy scan of a microresonator. (d) Resonance linewidth values (red - full linewidth, green - intrinsic loss rate, blue - coupling rate) (e) Extracted dispersion example of the hybrid microresonators. Inset shows a single resonance linewidth measurement with a sideband approach. (f) Histograms of intrinsic linewidth measurements of 2 different microring devices.

ment.

Platform performance

To analyze the optical loss, coupling properties, and group velocity dispersion (GVD) of hybrid structures, broadband frequency-comb-assisted spectroscopy is performed on multiple microresonators covering wavelength range of 1260-1630 nm (see Figure 1(c-f)). Individual microring resonators have quality factors up to 3×10^6, while photonic dimers exhibit quality factors up to 4.5×10^6. We associate the absorption peak at 1420 nm with an overtone of OH bonds in $LiNbO_3$. Optical losses increase with frequency due to increased radiation loss. Evanescent coupling is uniform over a span of 55 THz, and the dispersion can be adjusted by changing waveguide geometry or $LiNbO_3$ thickness. The presented design demonstrates uniform coupling over a broad frequency range and flat integrated dispersion.

To measure adiabatic transition efficiency and remove ambiguity from fiber-chip coupling loss, we designed an experiment with multiple breakouts on straight waveguides. Waveguides with 2, 4, 6, and 10 transitions were fabricated, and the increase in loss due to each transition was determined. As shown in Figure 2(d), each straight transition leads to approximately 1 dB loss, whereas the tapered input/output behaves as a virtually lossless transition. The authors observed an additional loss of approximately 0.8 dB for ten interfaces in the case of tapered transitions. Considering the statistical uncertainty, a transition loss of less than 0.1 dB per taper was deduced.

The precise lithography capabilities of the Si_3N_4 photonic circuit layer enable our heterogeneous integration approach to be versatile and robust. This is demonstrated by the implementation of a W-shaped 3-dB splitter/coupler that uses the hybrid Si_3N_4-$LiNbO_3$ mode, but is defined solely by underlying Si_3N_4 inverse tapers. Due to the presence of the $LiNbO_3$ slab and the single-mode nature of our hybrid waveguides, the optical mode is adiabatically transferred from the input arm to the output arms. The tapered sections are 100 μm long, ensuring a small footprint for integrated components exploiting this design. Transmission measurements of the device reveal a flat response, with power asymmetry between the two arms not exceeding 1.7 dB and on-chip insertion loss not exceeding 1 dB in the 1500-1620 nm wavelength range (Fig.2(f)).

Figure 2(h) shows the performance of a phase modulator, with a length of 4 mm (device image in Fig. 2(g)) and a confinement of 38%. Measuring the phase shift with the use of Mach-Zehnder interferometer we extract a V_π value of

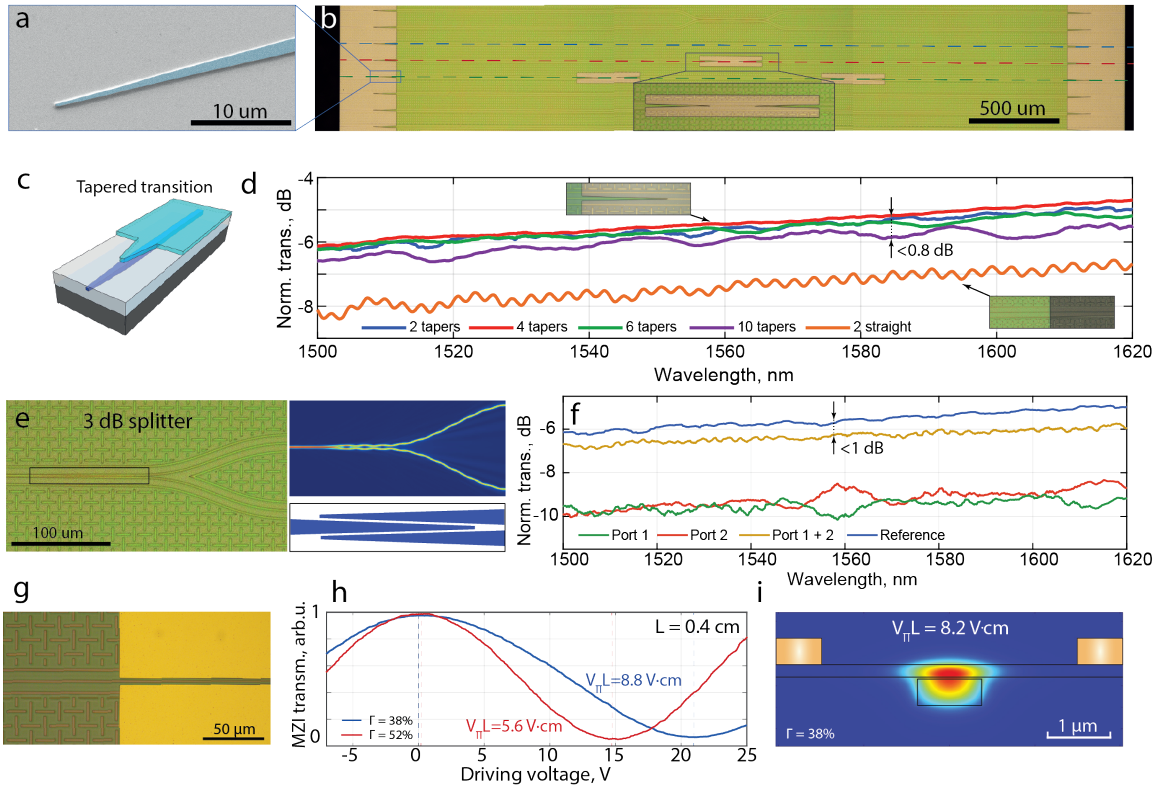

Fig. 2: (a) SEM image of an adiabatic tapered transition. (b) Microscope image of the text structures used to determine insertion losses of the platform. (c) Schematics of the coupling region. (d) Broadband transmission measurements of the test structures. (e) Schematics and simulations of a 3-dB splitter. (f) Transmission measurements of the fabricated 3-dB splitter. (g) Optical microscope image of a phase shifter used to determine the electro-optic performance. (h) Mach-Zehnder interferometer measurements of electro-optic response of the phase shifters. (i) Numerical simulations of the half-wave voltage of the platform.

22 V, which corresponds to the $V_\pi L$ product of approximately 8.8 V·cm (blue line). By reducing the Si_3N_4 waveguide width (therefore increasing the mode participation in the $LiNbO_3$ layer up to 52%) and decreasing the distance between electrodes down to 5.5 μm, we improve the electro-optic performance even further and achieve a $V_\pi L \sim 6$ V·cm (red line), however at the expense of optical losses.

Conclusions

In summary, we have developed a hybrid Si_3N_4-$LiNbO_3$ platform for photonic integrated circuits using direct wafer-scale bonding. This approach combines the low-loss Si_3N_4 technology with the second-order nonlinearity of $LiNbO_3$. We have also demonstrated a design for low-loss transitions from Si_3N_4 waveguides to hybrid Si_3N_4-$LiNbO_3$ waveguides. The achieved electro-optic performance is comparable to that of ridge waveguide structures, while keeping propagation losses independent of the quality of the $LiNbO_3$ etching. The platform's $V\pi L$ product value for phase modulators is approximately 8.8 V·cm. Our platform offers a range of applications, including photonic switching networks for neuromorphic or quantum computing, integrated electro-optic frequency comb sources, and on-chip generation of second-harmonic and squeezed light. This is the first time a heterogeneously integrated $LiNbO_3$ photonic platform combines all the beneficial features of Si_3N_4 PICs at wafer scale.

Acknowledgements

This work was supported by funding from the European Union Horizon 2020 Research and Innovation Program under the Marie Sklodowska-Curie grant agreement No. 722923 (OMT) and No. 812818 (MICROCOMB), as well as under the FET-Proactive grant agreement No. 732894 (HOT). This work was also supported by the Swiss National Science Foundation under grant agreement No. 176563 (BRIDGE) and 186364 (QuantEOM), as well as by Contract HR0011-20-2-0046 (NOVEL) from the Defense Advanced Research Projects Agency (DARPA), Microsystems Technology Office (MTO).

References

[1] I. Krasnokutska, J.-L. J. Tambasco, X. Li, and A. Peruzzo, "Ultra-low loss photonic circuits in lithium niobate on insulator", en, *Optics Express*, vol. 26, no. 2, p. 897, Jan. 2018, ISSN: 1094-4087. DOI: 10.1364/OE.26.000897. [Online]. Available: https://www.osapublishing.org/abstract.cfm?URI=oe-26-2-897 (visited on 05/05/2020).

[2] M. Zhang, C. Wang, R. Cheng, A. Shams-Ansari, and M. Lončar, "Monolithic ultra-high-q lithium niobate microring resonator", *Optica*, vol. 4, no. 12, pp. 1536–1537, Dec. 2017. DOI: 10.1364/OPTICA.4.001536. [Online]. Available: http://www.osapublishing.org/optica/abstract.cfm?URI=optica-4-12-1536.

[3] K. Luke, P. Kharel, C. Reimer, L. He, M. Loncar, and M. Zhang, "Wafer-scale low-loss lithium niobate photonic integrated circuits", *Optics Express*, vol. 28, no. 17, p. 24 452, Aug. 2020, ISSN: 1094-4087. DOI: 10.1364/OE.401959. [Online]. Available: https://ieeexplore.ieee.org/document/9252499/%20https://www.osapublishing.org/abstract.cfm?URI=oe-28-17-24452.

[4] B. Desiatov, A. Shams-Ansari, M. Zhang, C. Wang, and M. Lončar, "Ultra-low-loss integrated visible photonics using thin-film lithium niobate", *Optica*, vol. 6, no. 3, pp. 380–384, Mar. 2019. DOI: 10.1364/OPTICA.6.000380. [Online]. Available: http://www.osapublishing.org/optica/abstract.cfm?URI=optica-6-3-380.

[5] L. He, M. Zhang, A. Shams-Ansari, R. Zhu, C. Wang, and L. Marko, "Low-loss fiber-to-chip interface for lithium niobate photonic integrated circuits", *Optics Letters*, vol. 44, no. 9, p. 2314, 2019, ISSN: 0146-9592. DOI: 10.1364/ol.44.002314. arXiv: 1902.08969.

[6] P. Ying, H. Tan, J. Zhang, *et al.*, "Low-loss edge-coupling thin-film lithium niobate modulator with an efficient phase shifter", *Optics Letters*, vol. 46, no. 6, p. 1478, Mar. 2021, ISSN: 0146-9592. DOI: 10.1364/OL.418996. [Online]. Available: https://www.osapublishing.org/abstract.cfm?URI=ol-46-6-1478.

[7] P. O. Weigel, F. Valdez, J. Zhao, H. Li, and S. Mookherjea, "Lightwave circuits in lithium niobate through hybrid waveguides with silicon photonics", *Scientific Reports*, vol. 6, no. 1, p. 012 001, 2016. DOI: 10.1038/srep22301. [Online]. Available: https://doi.org/10.1038/srep22301.

[8] A. Rao, A. Patil, P. Rabiei, *et al.*, "High-performance and linear thin-film lithium niobate mach–zehnder modulators on silicon up to 50 ghz", *Opt. Lett.*, vol. 41, no. 24, pp. 5700–5703, Dec. 2016. DOI: 10.1364/OL.41.005700. [Online]. Available: http://opg.optica.org/ol/abstract.cfm?URI=ol-41-24-5700.

[9] S. Jin, L. Xu, H. Zhang, and Y. Li, "Linbo3 thin-film modulators using silicon nitride surface ridge waveguides", *IEEE Photonics Technology Letters*, vol. 28, no. 7, pp. 736–739, 2016. DOI: 10.1109/LPT.2015.2507136.

[10] J. Liu, G. Huang, R. N. Wang, *et al.*, "High-yield, wafer-scale fabrication of ultralow-loss, dispersion-engineered silicon nitride photonic circuits", *Nature Communications*, vol. 12, no. 1, p. 2236, 2021. DOI: 10.1038/s41467-021-21973-z. [Online]. Available: https://doi.org/10.1038/s41467-021-21973-z.